Escola de Primavera de Transição e Turbulência
Blumenau 2022

13th Spring School on Transition and Turbulence
September 19th-23rd, 2022, Blumenau, SC, Brazil

EPTT-2022-0057
EROSION IN SQUARE-SHAPED AND AERODYNAMICS BAFFLES IN GAS-SOLID FLOW OF A CFB RISER: COMPARISON USING DIFFERENT EROSION MODELS

Vivien Rossbach
Arthur B. A. Bernardo
State University of Campinas - Campinas, Brazil
vrossbach@furb.br
a231638@dac.unicamp.br

Sarah L. Becker
Henry França Meier
University of Blumenau – Blumenau, Brazil
sarahlaisa@gmail.com
meier@furb.br

Dirceu Noriler
State University of Campinas - Campinas, Brazil
dnoriler@unicamp.br

Abstract. *Using ring baffles has been widely discussed to increase the gas-solid contact in CFB risers. Several optimized geometries for ring-baffles have been proposed in the literature to improve the solids dispersion without causing a large axial pressure drop in the riser. However, it is necessary to consider the erosion suffered by ring baffles because of the impingement of solid particles on their surface to estimate their life cycle. This study evaluates, through CFD simulations, the temporal and local erosion suffered by aerodynamic and square-shaped ring-type baffles in a pilot-scale CFB riser. These baffles, according to the literature, have a better performance in increasing gas-solid contact in CFB risers. Four different erosion models were compared to quantify erosion using an Eulerian-Lagrangian approach and the Finnie model presented the best results. The use of both baffle types increased the erosion in the riser outlet, and the global erosion of the squared baffles is greater than that of the aerodynamic ones. Finally, aerodynamic baffles presented the lowest erosion rates along the riser but increased the erosion in the T-outlet.*
Keywords: *Computational Fluid Dynamics (CFD), Erosion, Ring-baffles, CFB riser.*

1. INTRODUCTION

Circulating fluidized beds (CFB) are equipment used in different industrial applications, like fluid catalytic cracking (FCC) (Li et al., 2014), ozone decomposition (Jiang et al., 1991), and dehydrogenation (Kashyap et al., 2020), and CFB combustors (Zhou et al., 2013). In the main section of the CFB unit is located the riser reactor, where fast catalytic reactions occur in a turbulent upward gas flow (Wang et al, 2014). The core-annulus profile formation observed near the riser wall must be avoided because it decreases the gas-solid contact and the yield of chemical reactions (Lopes et al., 2011). Several devices have been proposed for this purpose, such as gas and solids distributors (Therdthianwong et al., 2003), internal baffles (Rossbach et al., 2016; Samruamphianskun et al., 2012), and the use of acoustic waves on the riser wall (Rossbach et al., 2020). Among these alternatives, the internal baffles stand out in several industrial applications. Different geometrical shapes were proposed for the baffles in the literature, such as square-shaped baffles (Samruamphianskun et al., 2012; Wang et al., 2019), wedged baffles (Guío-Pérez et al., 2014), triangular-shaped baffles (Wells, 1998; Dries, 2003), trapezoidal-shaped ones (Mehlberg and Sandacz, 2014), and airfoil-shaped ring-type baffles (Rossbach et al., 2019).

The ring-baffles used in CFB risers must have their shape optimized to be applied in industrial processes. The optimization processes contribute to finding a configuration that provides a better solids dispersion, increases the yield of chemical reactions, and minimizes the pressure drop and the erosion of the baffle surface (Jiang et al., 1991). Erosion in riser internals occurs due to the impact of solid particles subject to deformation and breakage during the flow in the fluidized bed (Mehrani and Sowinski, 2020). Several types of equipment inside a circulating fluidized bed are subject to erosion, such as distributors, heat exchanger ducts, cyclones, and riser internals. Inner baffles are commonly found in applications with fast fluidization regimes and pneumatic transport (Basu, 2006).

Erosion depends on both operational conditions and solid particle properties (Chu et al., 2014), and is greater in the regions where gas and solids velocity is higher, such as in the distributors, in the inlet of cyclones (Mehrani and Sowinski, 2020), and inside the ring-baffled riser (Jiang et al., 1991). Wang et al. (2019) conducted a numerical study of the influence of square-shaped ring baffles on the gas-solid flow in a CFB riser and observed a reverse flow above the baffle placed near the riser outlet, which indicates that the baffle will suffer severe erosion. In contrast, the wedged baffles proposed by Guío-Perez et al. (2014) have a smoother slope compared to the square-shaped ones and avoided the formation of dead zones in their upper and lower regions. Likewise, the airfoil-shaped ring-baffles proposed by Rossbach et al. (2019) avoided the formation of dead zones, delaying the detachment of the boundary layer from their surface.

This study aims to investigate the erosion in CFB risers with aerodynamic and square-shaped ring-type baffles through numerical simulations, and relate the turbulence with the erosion flux in baffled CFB risers. Four erosion models were investigated – DNV, Finnie, Oka, and McLaury – and the erosion rates estimated with these models were compared with experimental data. The erosion of aerodynamic and square-shaped ring-type baffles in the CFB riser was investigated using the model that presented the best estimation. Also,we investigated the relation between the turbulence kinetic energy distribution and the erosion flux with aerodynamic and squared baffles.

2. MATHEMATICAL MODEL

An Eulerian-Lagrangian approach was employed to keep the simulations of this study, based on the model proposed by Sedrez et al. (2017). The $\kappa - \varepsilon$ model with Enhanced Wall Treatment was used to describe the turbulence of the gas phase. Equations of the turbulence model can be found in Rossbach et al. (2021). Four models implemented in the commercial code Ansys FLUENT© 19.1 (Ansys Inc., 2020) were compared in this study. In the Finnie erosion model, the erosion rate is described by

$$E_{Finnie} = kV_P^n f(\gamma) \tag{1}$$

where E is a dimensionless erosion mass, k is a model constant, V_P is the particle impact velocity, and $f(\gamma)$ is a function of the angle of impact γ. The function $f(\gamma)$ is calculated as:

$$f(\gamma) = \{\tfrac{1}{3}\gamma \ for\, \gamma > 18.5° \ \sin sin\,(2\gamma) \ - 3\gamma \ for\, \gamma \leq 18.5° \tag{2}$$

The erosion rate is calculated by the Oka model as:

$$E_{Oka} = E_{90}\left(\frac{v}{v_{ref}}\right)^{k_2}\left(\frac{d}{d_{ref}}\right)^{k_3} f(\gamma) \tag{3}$$

where E_{90} is the reference erosion rate at 90° angle of impact, v is the particle impact velocity, v_{ref} is the reference velocity, d is the particle diameter and d_{ref} is the particle reference diameter, k_2 and k_3 are the velocity and diameter exponents. The dependence of the erosion rate with the impact angle is given by:

$$f(\gamma) = (\sin sin\,\gamma\,)^{n_1}\left(1 + H_v(1 - \sin sin\,\gamma\,)\right)^{n_2} \tag{4}$$

where γ is the wall impact angle, in rad, H_v is the Vickers hardness, in GPa, n_1 and n_2 are constants. The standard values referenced in the Ansys FLUENT Theory Guide (Ansys Inc., 2020) were used in this study because of the similarity of the materials.

The erosion model proposed by McLaury is proper to solid-liquid flows with water and sand particles, like that found in slurry reactors. The erosion rate is given by:

$$E_{McLaury} = Av^n f(\gamma) \tag{5}$$

where

$$A = F\, Bh^{k} \tag{6}$$

In Eqs. 5 and 6, F is an empirical constant, v is the particle impact velocity, Bh is Brinell's hardness of the wall, and $k = -\ 0.59$ is a constant calculated for carbon steel. The function $f(\gamma)$ is given by:

$$f(\gamma) = \{b\gamma^{2} + c\gamma\ for\ \gamma \leq \gamma_{lim}\ x\gamma\ \sin sin\,(w\gamma)\ +\ y(\gamma)\ +\ z\ for\ \gamma > \gamma_{lim} \tag{7}$$

The standard values presented in the Ansys FLUENT© Theory Guide (Ansys Inc., 2020) were used for the calculations. The DNV erosion model calculates the erosion rate as

$$E_{DNV} = k v_{p}^{n} f(\gamma) \tag{8}$$

where n is a material-dependent velocity exponent, k is an empirical constant given in $\left[\left(\frac{m}{s}\right)^{-n}\right]$, v_p is the particle impact velocity, in m/s, and, for steel, $f(\gamma)$is given by:

$$f(\gamma) = \sum_{i=1}^{8} (-\ 1)^{i+1} A_{i} \gamma^{i} \tag{9}$$

Also for the DNV model, the standard values provided by the Ansys FLUENT© Theory Guide (Ansys Inc., 2020) for the steel were adopted.

3. METHODOLOGY

Figure 1-a,e shows the geometry of the CFB riser, with a height of 15.5 m, an inner diameter of 0.1 m, and a gas and solids outlet with an inclination of 10° concerning the solids inlet. In addition, the solids inlet inclines 45° regard the vertical direction. The geometrical parameters of the aerodynamic and the square-shaped ring baffles are indicated in Fig. 1-f.g, respectively. Both have a thickness of 2.57 mm and the difference between them is the angle of inclination. The aerodynamic baffles have a 43.62° angle of impact and the squared baffles have a 90° angle of impact.

Three cases were simulated: the riser without baffles, the riser with 22 aerodynamic-shaped baffles, and the riser with 22 square-shaped baffles. In the last cases, 22 baffles were placed along with the riser height, as indicated in Fig. 1-a. The criteria for the axial distancing of the baffles was the visual identification of the positions in which the solid particles tend to accumulate near the wall. One ring-baffle was inserted in each position identified. The first baffle is located 15 cm above the solids inlet. The lowest baffles are distanced by 10 cm, 15 cm, 30 cm, and 50 cm, respectively, and the last three baffles near the outlet have a distance of 15 cm between them. The baffles in the intermediate region of the riser have a distance of 1 m between them. The aerodynamic-shaped geometry was proposed by Rossbach et al. (2016; 2019) and the square-shaped geometry is based on the study of Samruamphianskun et al. (2012). The hexahedral mesh of unstructured blocks In Fig. 1-b,c, and d have 737,000 elements. A study of grid dependence for this mesh was performed by Utzig (2016) for the riser without baffles, and the meshes for the baffled riser have a global y^{+} value of 73.

The experiments and the simulations were performed adopting a gas velocity of 10 m/s and a solids mass flux of 4.21 kg/m²s. For each case, we performed 10 s of simulations, with the transient mean values taken at the last 5 s. A time step of 0.0001 s was adopted, and the convergence criteria for the residuals were defined as 0.0001. The simulations were realized in the commercial code Ansys FLUENT 19.1 for 15 days, using 12 cores. The gas phase is represented by air at ambient conditions. Otherwise, the solid particles are FCC catalyst particles with a density of 1500 kg/m³, a mean diameter of 67 µm, and a Rosin-Rammler distribution, with a spreading factor of 6.9, 10 classes of diameters, and a shape factor equal to 1. To get the erosion rates in [kg/h] to compare with the experimental results, we multiplied the post-processed values, given in [kg/m²], by 3600 s and by the cross-sectional area of the rings, and divided the results by 10 s, that was the simulated operating time.

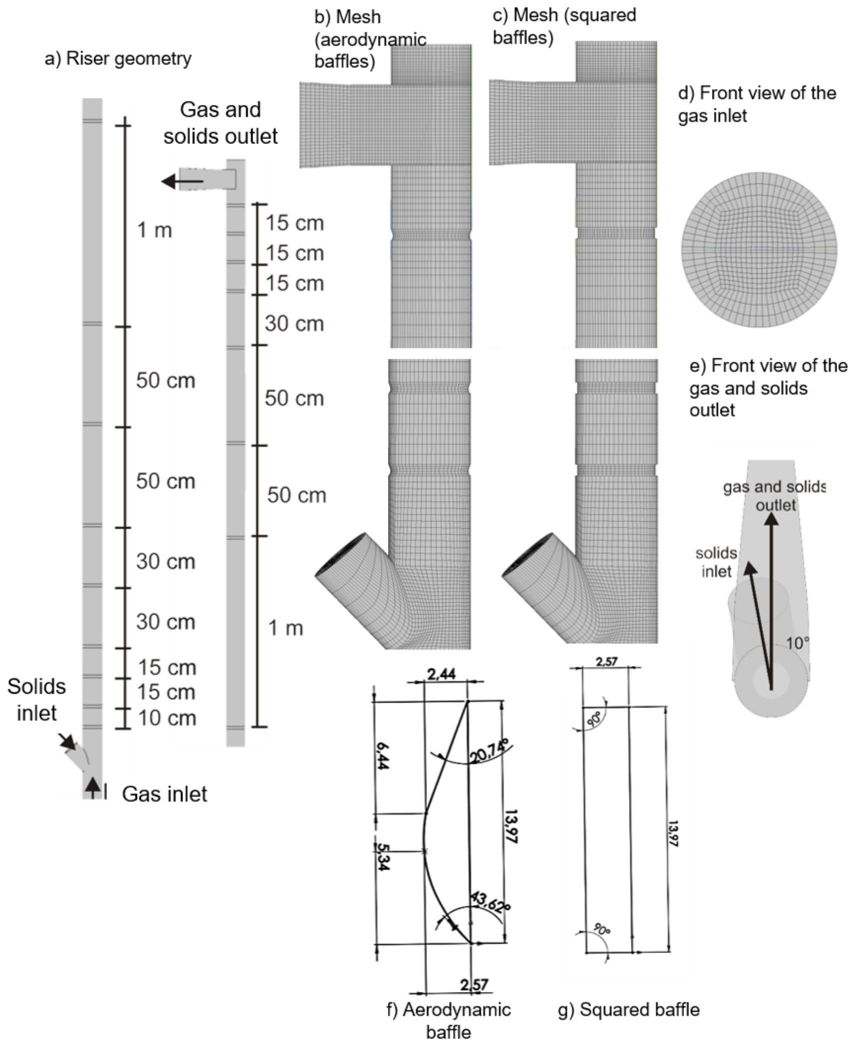

Figure 1. Geometry and mesh of the CFB riser and the ring-type baffles: a) riser geometry, b) mesh of the riser with aerodynamic baffles; c) mesh of the riser with squared baffles, d) front view of the gas inlet, e) front view of the gas and solids outlet, f) geometrical parameters of the aerodynamic baffle, g) geometrical parameters of the squared baffle.

4. RESULTS AND DISCUSSION

The erosion rates estimated by the four erosion models were compared with experimental data from Rossbach et al. (2021). The experimental erosion rate was obtained for aerodynamic-shaped ring baffles with the same geometry as this study. As the baffles were made from gypsum with known hardness, appropriate correlations were employed to relate this value with the erosion rate of a stainless steel-made baffle. According to the results of Table 1, only the erosion rate estimated by the DNV model is very different from the experimental result. Finnie, McLaury, and Oka's models provided predictions with a relative error of 44%, 110%, and 152%, respectively. If we choose the Finnie model, the simulated erosion rate of the squared-shape baffles for this operating condition is 12.80 g/h, which is a very higher value. Even though this rate is probably overestimated, square-shaped baffles present much more erosion than the aerodynamics one in the same operating condition. It occurs because squared baffles have an inclination of 90° concerning the up flow and the aerodynamic baffles have a soft angle of inclination that avoids the detachment of the laminar boundary layer and prevent flow instabilities that lead to erosion. It is important to highlight that the error of using McLaury model here is attributed to the fact that this model was developed for gas-liquid flows with sand particles, and we are using only gas flow with FCC particles.

Table 1 – Comparison of the erosion rates of the simulations with the experimental result.

Erosion rate (g/h)				
Experimen t	DNV model	Finnie model	McLaury model	Oka model
7.63E-03	2.29E-07	1.10E-02	1.60E-02	1.93E-02
Error	100 %	44 %	110 %	152 %

Figure 2 shows the temporal series of the erosion flux for the aerodynamic and the square-shaped ring baffles during the simulations. As the vertical axis is presented in a logarithmic shape, we can see that the erosion flux increase in the beginning and tends to stabilize in both cases. However, the erosion flux is higher for the squared baffles.

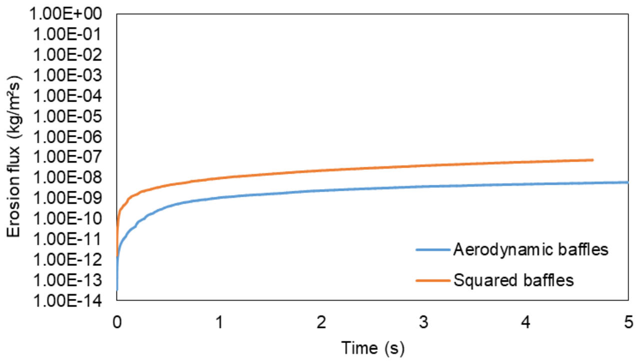

Figure 2. Erosion in aerodynamic and square-shaped baffles placed in the CFB riser using the Finnie model.

Figure 3-a shows the erosion flux in the riser wall and Fig. 3-b shows the erosion only on the surface of the baffles. In Fig.1-a we can observe that the erosion flux in the baffles is much lower than in the wall. In the region immediately above the solids inlet, the erosion flux increases slightly. Conversely, the erosion in the T-outlet increases with the presence of both types of baffles. This region suffers severe erosion even without baffles, as pointed out by Rossbach et al. (2021b). In this case, whichever type of baffle is used, its placement at the top must be redesigned to avoid T-outlet erosion.

In Fig. 3-b, the erosion of the baffles was highlighted in the inlet and outlet regions of the riser, as we did in the other images because these regions have the largest erosion flux. The first aerodynamic baffle above the solids inlet has severe erosion compared to the next, but the erosion flux rapidly decreases with the riser height. Otherwise, the erosion in the squared-baffles is also severe and does not reduce with the riser height. The last two squared baffles before the riser outlet has lower erosion flux, but the baffles below them have a higher erosion due to the backmixing. In the riser with aerodynamic baffles, the erosion flux is well distributed between the baffles near the riser outlet.

Even though the objective of this study is to investigate the erosion flux in the ring baffles, to estimate their life cycle in an industrial CFB riser, the results observed in Fig. 3 allow us to conclude that using ring baffles near the riser outlet increases the erosion flux in the riser T-outlet. This occurs because the reduction of the opening area leads to an increase in the flow velocity and the turbulent energy dissipated in the T-outlet region. This trend was observed for both aerodynamic and squared baffles. So, using ring baffles benefits the solids distribution in the inlet region, but using these devices near the outlet can reduce not only the ring baffles life cycle, but the riser life cycle.

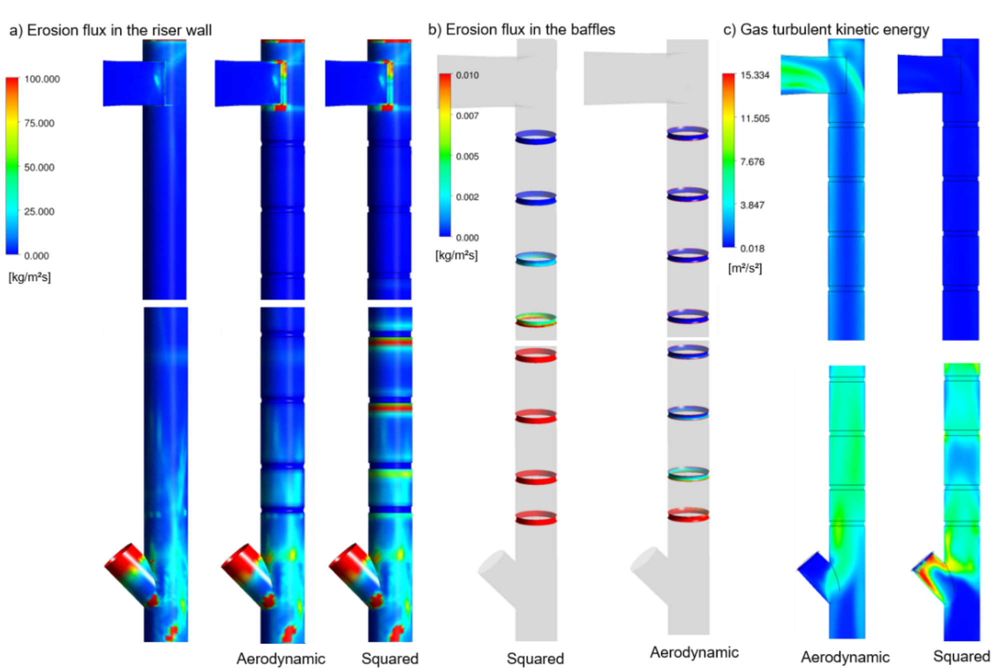

Figure 3. Erosion in the riser wall (a), erosion in the baffles (b), and gas turbulent kinetic energy (c).

According to Rossbach et al. (2019), the particle velocity in the CFB riser increases with the presence of ring baffles because they reduce the opening area of the riser. Consequently, turbulence increases where the baffles were placed. Figure 3-c compares the distribution of the turbulent kinetic energy in the CFB riser with aerodynamic and square-shaped baffles with aims to relate the turbulence with the erosion flux. The turbulent kinetic energy is well distributed along the inlet region of the riser with aerodynamic baffles than in the case with square-shaped baffles. In the outlet region, the turbulent energy values are lower for the riser with square-shaped baffles, which could imply that more flow energy was dissipated than in the case with aerodynamic baffles, leading to more backmixing. The better distribution of the turbulent energy in the top of the riser with aerodynamic baffles can be related to the well-distributed erosion flux in the baffles placed in this region.

5. CONCLUSIONS

This study investigated the erosion in a pilot-scale CFB riser with aerodynamic and square-shaped ring-type baffles subjected to a gas-solid flow, under turbulent conditions. Numerical simulations were conducted using an Eulerian-Lagrangian approach to compare the erosion rates estimated with DNV, McLaury, Oka, and Finnie erosion models. Finnie erosion model presents the best result, i. e. 44% of error, compared to experimental data for aerodynamic baffles, and was chosen to compare the erosion flux in the CFB riser with aerodynamic and square-shaped baffles. The aerodynamic baffles present a lower and well-distributed erosion flux along with the riser height when compared to the square-shaped baffles. The aerodynamic baffles presented an en flux near 10^{-10} kg/m²s, while the squared baffles presented an erosion flux around 10^{-8} kg/m²s. In addition, both baffled-riser configurations increased the erosion of the T-outlet compared to the riser without baffles. Thus, more investigations are necessary to adjust the position of the baffles near the riser outlet, to avoid T-outlet erosion.

6. ACKNOWLEDGEMENTS

The authors are grateful for the financial support from the Human Resources Program of the National Agency for Petroleum, Natural Gas and Biofuels – PRH-ANP, supported with resources from the investment of oil companies qualified in the P, D&I Clause of ANP Resolution 50/2015, through the process Nº043919.

7. REFERENCES

Ansys Inc., 2020. “ANSYS FLUENT Theory Guide.” ANSYS Inc., USA. Vol. Release 20.

Basu, P., 2006. Combustion and Gasification in Fluidized Beds. CRC Press. https://doi.org/10.1201/9781420005158.

Chu, K. W., S. B. Kuang, A. B. Yu, A. Vince, G. D. Barnett, and P. J. Barnett., 2014. “Prediction of Wear and Its Effect on the Multiphase Flow and Separation Performance of Dense Medium Cyclone.” Minerals Engineering 56: 91–101. https://doi.org/10.1016/j.mineng.2013.10.029.

Dries, H. W. A., 2003. Reactor riser of a fluidized-bed catalytic cracking plant. US no 6,596,242 B1, issued 2003.

Guío-Pérez, D. C., T. Pröll, and H. Hofbauer. 2014. “Influence of Ring-Type Internals on the Solids Residence Time Distribution in the Fuel Reactor of a Dual Circulating Fluidized Bed System for Chemical Looping Combustion.” Chemical Engineering Research and Design 92 (6): 1107–18. https://doi.org/10.1016/j.cherd.2013.10.018.

Jiang, P., Bi, H., Jean, R. H., and Fan, L. S., 1991. “Baffle Effects on Performance of Catalytic Circulating Fluidized Bed Reactor.” AIChE Journal 37 (9): 1392–1400. http://www.scopus.com/inward/record.url?eid=2-s2.0-0026223383&partnerID=tZOtx3y1.

Kashyap, Mayank, Malleswara Rao Tadiboyina, Christian Okolo, and Sami Al-Mutairi. 2020. “Improving Circulating Fluidized Bed Dehydrogenation Technology through Optimization of Fluidization.” Particuology 50 (June): 127–34. https://doi.org/10.1016/j.partic.2019.07.007.

Li, Z., Wang, L., Yang, C., and Li, C., 2014. “Effect of Ring-Feeder Form of FCC Riser on Gas-Solids Flow Structure.” Petroleum Processing and Petrochemicals 45 (1): 47–50. http://www.scopus.com/inward/record.url?eid=2-s2.0-84893771134&partnerID=tZOtx3y1.

Lopes, G. C., Rosa, L. M., Mori, M., Nunhez, J. R., and Martignoni, W. P., 2011. “Three-Dimensional Modeling of Fluid Catalytic Cracking Industrial Riser Flow and Reactions.” Computers and Chemical Engineering 35 (11): 2159–68. https://doi.org/10.1016/j.compchemeng.2010.12.014.

Mehlberg, R. L., and Sandacz, M. S., 2014. Segmented baffle system for a riser. US20140356248A1, issued 2014.

Mehrani, Poupak, and Andrew Sowinski. 2020. “Operating Challenges.” In Essentials of Fluidization Technology. https://doi.org/10.1002/9783527699483.ch13.

Rossbach, V., Utzig, J., Decker, R.K., Noriler, D., Soares, C., Martignoni, W.P., and Meier, H.F., 2019. “Gas-Solid Flow in a Ring-Baffled CFB Riser: Numerical and Experimental Analysis.” Powder Technology 345. https://doi.org/10.1016/j.powtec.2018.12.096.

Rossbach, V., Padoin, N., Meier, H. F., and Soares, C., 2020. “Influence of Acoustic Waves on the Solids Dispersion in a Gas-Solid CFB Riser: Numerical Analysis.” Powder Technology 359 (January): 292–304. https://doi.org/10.1016/j.powtec.2019.09.075.

Rossbach, V., Padoin, N., Meier, H. F., and Soares, C., 2021. “Influence of Ultrasonic Waves on the Gas-Solid Flow and the Solids Dispersion in a CFB Riser: Numerical and Experimental Study.” Powder Technology 389: 430–49. https://doi.org/10.1016/j.powtec.2021.05.051.

Rossbach, V., Utzig, J., Decker, R. K., and Meier H. F., 2021. “Projeto V&VinCFD – FASE II: Desenvolvimento de ‘Benchmarks’ Para Verificação e Validação Em CFD de Escoamentos Multifásicos Da Indústria Do Refino de Petróleo,” 57.

Rossbach, V., Utzig, J., Decker, R. K., Noriler, D., and Meier, H. F., 2016. “Numerical Gas-Solid Flow Analysis of Ring-Baffled Risers.” Powder Technology. https://doi.org/10.1016/j.powtec.2016.04.044.

Samruamphianskun, T., Piumsomboon, P., and Chalermsinsuwan, B., 2012. “Effect of Ring Baffle Configurations in a Circulating Fluidized Bed Riser Using CFD Simulation and Experimental Design Analysis.” Chemical Engineering Journal 210: 237–51. https://doi.org/10.1016/j.cej.2012.08.079.

Sedrez, T. A., Decker, R. K., da Silva, M. K., Noriler, D., and Meier, H. F., 2017. “Experiments and CFD-Based Erosion Modeling for Gas-Solids Flow in Cyclones.” Powder Technology 311: 120–31. https://doi.org/10.1016/j.powtec.2016.12.059.

Therdthianwong, A., Pantaraks, P., and Therdthianwong, S., 2003. “Modeling and Simulation of Circulating Fluidized Bed Reactor with Catalytic Ozone Decomposition Reaction.” Powder Technology 133 (1–3): 1–14. https://doi.org/http://dx.doi.org/10.1016/S0032-5910(03)00120-7.

Utzig, J., 2016. “Particle Phase Dynamics in a Circulating Fluidized Bed.” Federal University of Uberlandia.

Wang, C., Zhu, J., and Barghi, S., 2014. “Catalytic Ozone Decomposition in High Density Gas-Solids Circulating Fluidized Bed Riser and Downer Reactors.” In CFB-11: Proceedings of the 11th International Conference on Fluidized Bed Technology, 73–78. Chemical Industry Press. http://www.scopus.com/inward/record.url?eid=2-s2.0-84902679459&partnerID=tZOtx3y1.

Wang, S., Luo, K., Hu, C., and Fan, J., 2019. “CFD-DEM Study of the Effect of Ring Baffles on System Performance of a Full-Loop Circulating Fluidized Bed.” Chemical Engineering Science. https://doi.org/10.1016/j.ces.2018.10.056.

Wells, J. W., 1998. Process and apparatus for fluidized catalytic cracking of a hydrocarbon feed. US no 5,851,380, issued 1998.

Zhou, W., Zhao, C., Duan, L., Chen, X., and Liu D., 2013. “A Simulation Study of Coal Combustion under O2/CO2 and O2/RFG Atmospheres in Circulating Fluidized Bed.” Chemical Engineering Journal 223: 816–23. https://doi.org/10.1016/j.cej.2013.03.051.

8. Responsibility notice

The authors are the only ones responsible for the printed material included in this paper.